

# A numerical model approach of wave dynamic

Muhammad Irham<sup>1,2,3,\*</sup>, Yopi Ilhamsyah<sup>1</sup>, Edy Miswar<sup>1,2,3,4</sup>

<sup>1</sup> Department of Marine Science, Faculty of Marine and Fisheries, Universitas Syiah Kuala University, 2311, Indonesia

<sup>2</sup> Center for Environmental and Natural Resources Research, Universitas Syiah Kuala

<sup>3</sup> Geographic Information Systems Laboratory, Faculty of Marine and Fisheries Science, Universitas Syiah Kuala

<sup>4</sup> Department of Fisheries Resources Utilization, Faculty of Marine and Fisheries, Universitas Syiah Kuala, Banda Aceh, 2311, Indonesia

**Abstract.** The numerical model of wave field distribution using time dependent of wave combination from refraction-diffraction equation on a gentle slope was carried out in Modeling Laboratory of Marine and Fisheries Faculty of Syiah Kuala University. The research of numerical modeling was conducted to understand how the impact of the presence of coastal structures on the coast toward the wave dynamic approach. In the theory, the greater of wave angle, the greater of wave height distribution will be behind the breakwater, thus allowing large sediment transport to make changes to the coast. Therefore, this research is important because the knowledge of the relationship between waves and coastal structure is still limited while the dynamics of the coast have a distinctive significance in the regions. The study aims to determine the wave phenomena that interact with the structure of the coastal building so that the results of this study can be used and utilized as substantial study for future coastal planning. The method used in this study is the application of wave equations that may be solved by numerical model. The model results show that the greater the angle of incidence of waves on the southwest coast, the greater the wave height produced when it hits coastal structures. However, this characteristic does not occur in the west coast region. This is caused by the topographic nature of coastal areas and different coastal characteristics.

## 1 Introduction

Coastal areas have a significant role in human life, such as the use of marine reserves as a source of food, medicine, transportation, and recreation [1]–[4]. Coastal waters are also vulnerable to various human activities through extensive tourism activities, fishing, ports, [4] and industrial estate development [5]. As a result, industrial development which is directly proportional to the increase in pollutants from time to time causes physical and ecological changes in coastal areas and their surroundings [2]. It is important to study the interactions between the coast and the ocean to understand these changes. A beach usually has significant

---

\* Corresponding author: [iham@usk.ac.id](mailto:iham@usk.ac.id)

wave characteristics due to non-linear interactions in shallow water depths [6]. Waves trigger the transport, dispersion, and vertical mixing of seawater such as fronts and particle transport [7]. Strong wave-induced currents can cause erosion of seafloor sediments and maintain the shape of the sediment in suspended particles [8], [9]. However, waves and currents vary across the coasts of the world depending on their interactions with coastal geometry, bedtime bathymetry, and wave superposition [10].

The coastal area is unique because of the geographical location of the ocean [11]. In addition, this area is also strongly influenced by the topography of the area around the coast [12]. The topography of the mountainous areas bordering the sea is quite significantly different from the coasts in the lowland valleys and basins [13]. These factors are characteristics that affect the nature of wave propagation and its interaction with coastal waters [14]. The wave propagation interacts with coastal topography having unique wave dynamics [15]. The presence of shoaling is caused by the bathymetric profile of the beach towards the coastal area causing diffraction and refraction of the distribution of waves which causes the supply of energy through divergence due to the influence of forces acting on the coastal topography.

Studies on wave propagation in coastal areas are still lacking, especially in the coastal areas of Aceh. There have been several studies of waves on the coast of Aceh which have been reported in several articles. [11] reported that there were coastal waves that triggered longshore currents around Lhok Nga beach. [16]–[18] reported that seasons determine the flow and transportation of suspended sediments in the northern waters of Aceh. [15] reported that in the waters of West Aceh the influence of wind on currents is quite small, especially during the transition of seasons. Coastal waters have a rough bottom topography and a varied coastline. This condition causes the influence of waves on current circulation to be relatively complex compared to open water [19]. Considering that studies on the propagation of waves are still of minimal importance while an understanding of waves can be useful for environmental mitigation, especially for waters that are busy with industrial activities and waste [13], this study can be used as a solution to answer this challenge.

In line with efforts to utilize marine resources, while still paying attention to environmental sustainability and carrying capacity, knowledge, and technology and the meaning of marine research need to be increased. The fact that research on the sea in the last few decades has been carried out more to support the utilization and conservation of the sea and coastal areas. To fulfil this goal, several studies in coastal areas have focused more on the ecological role of bio-physical-chemical properties where the three subjects are interrelated. On the marine physics side, the interaction of hydro-oceanography with the coast is one of the most important studies to be carried out, especially regarding the interaction and propagation of waves along the coast to see the nature and characteristics of the dynamics that occur. Therefore, the study of wave propagation on the coast is an important focus in this study to find out how wave propagation and wave trajectories in this area react to aspects of coastal geomorphology and hydro-oceanographic dynamics.

## **2 Material and Methods**

### **2.1 Numerical Method**

The study used numerical method based on equations of shoaling and refraction of wave, which have been established by [11], [15], while the input data is obtained from field measurements made during high and low tide.

The numerical wave equations solution will be solved by discretizing the equation of wave (12) which comprises the coefficients of shoaling and refraction from (13), (14), and

(15). Based on wave equation, the wave height can also be calculated by applying the equation below [19].

$$H = H_0 K_s K_r \tag{1}$$

In which  $H$  and  $H_0$  are wave and initial wave height respectively,  $K_s$  shoaling coefficient, and  $K_r$  is refraction coefficient.

## 2.2 Discretization of Equations

The Applying the central difference approach, the equation (13) can be obtained as:

$$\beta^{n+1} = \frac{(p_t \Delta t - 2)\beta^{n-1} + (4 - 2q_t \Delta t^2)\beta^n}{(2 + p_t)} \tag{18}$$

with

$$p_t = -\frac{\partial c^n}{\partial x} \cos \theta^n + \frac{\partial c^n}{\partial y} \sin \theta^n \tag{19}$$

$$q_t = c^n \left( \frac{\partial^2 c^n}{\partial x^2} \sin^2 \theta^n - \frac{\partial^2 c^n}{\partial x \partial y} \sin 2\theta^n + \frac{\partial^2 c^n}{\partial y^2} \cos^2 \theta^n \right) \tag{20}$$

While the governing equation used as numerical approach is the wave form Equation (12):

$$\theta^{n+1} - \theta^n = \frac{\Delta s}{c^n} \left( \sin \theta^n \frac{dc^n}{dx} - \cos \theta^n \frac{dc^n}{dy} \right) \tag{21}$$

where  $\frac{dc}{dx} = \frac{c_{i+1,j} - c_{i-1,j}}{\Delta x_i + \Delta x_{i+1}}$  and  $\frac{dc}{dy} = \frac{c_{i,j+1} - c_{i,j-1}}{\Delta y_j + \Delta y_{j+1}}$  (22)

Here, the tangential component of the wave path in equation (10 and 11) will use the position of the new wave trajectory point which is discretized as:

$$x^{n+1} = x^n + \Delta s \cos \left( \frac{\theta^{n+1} + \theta^n}{s} \right) ds \tag{23}$$

$$y^{n+1} = x^n + \Delta s \sin \left( \frac{\theta^{n+1} + \theta^n}{s} \right) ds \tag{24}$$

where  $\Delta s = \Delta t \cdot c^n$ .

with point of  $x^n$ ,  $y^n$ ,  $x^{n+1}$ , and  $y^{n+1}$  do not have to have a grid value.

To attain the distribution of the wave trajectory multiply (23 and 24) by interpolating the points in a grid (**Figure 3**). The interpolation formulation used is

$$c^n = c_{i,j}(\zeta - 1)(\eta - 1) - c_{i+1,j}(\zeta)(\eta - 1) - c_{i+1,j+1}(\zeta)(\eta) + c_{i,j+1}(\zeta - 1)(\eta). \tag{25}$$

Where  $x^n$ ,  $y^n$ ,  $x^{n+1}$ , and  $y^{n+1}$  are the positions of  $x$  and  $y$  at  $n$  and  $n+1$  time step respectively,  $\beta^{n-1}$ ,  $\beta^n$  and  $\beta^{n+1}$  are orthogonal coefficients at  $\beta$  at  $n-1$ ,  $n$ , and  $n+1$  time step,  $\theta^n$  and  $\theta^{n+1}$  are wave angle at  $n$  and  $n+1$  time step,  $i$ ,  $i+1$ ,  $i-1$ , and  $j$ ,  $j+1$ ,  $j-1$  are distance position on grid  $x$  and  $y$  at distance step,  $\Delta x$ ,  $\Delta y$ ,  $\Delta t$ , and  $\Delta s$  are the grid spaces of  $x$ ,  $y$ ,  $t$ , and  $\zeta$  and  $\eta$  the elevation factor toward  $x$  and  $y$  grid called staggered mesh scheme (SMS) as shown in **Figure 1** below.

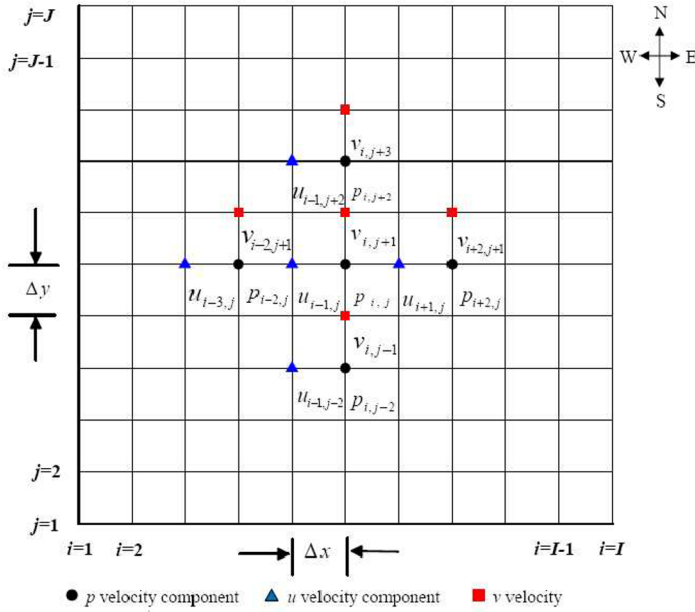


**Fig. 1.** Staggered Mesh Scheme.

### 2.3 Model Design

The numerical model of ocean waves is built on a gentle slope equation, the input of wave parameters such as incoming wave height ( $H_0$ ), period ( $T$ ), wave angle of arrival and the bathymetry. While the program results are in the form of wavelength ( $L$ ), phase speed ( $C$ ), wave group speed ( $C_g$ ), wave number ( $k$ ), refraction coefficient ( $K_r$ ), trajectory position ( $x_x, y_x, y_y$ ), elevation ( $\zeta$ ), and wave height ( $H$ ).

In the wave field distribution model is done by using equation (9), where in the simulation, the effect of a wave break is calculated by its energy dissipation factor ( $f_D$ ). The  $f_D$  energy dissipation factor is first to set zero (0) then given a value when the wave enters the break area, the size depends on the breaking wave coefficient. When waves reach the beach and coastal structure, the reflectivity is applied as the reflection coefficient ( $K_r$ ). The higher the  $K_r$ , the higher the reflected wave in the coastal boundary and coastal structure.

## 3 Result and Discussion

### 3.1 Bathymetry Digitization Results

Based on the results of the bathymetric analysis carried out, the deepest depth data obtained in the study in Gampong Suak Puntong, Kuala Pesisir sub-district, Nagan Raya Regency is 18 meters, which is located between Suak Puntong Village, Nagan Raya Regency and Peunagan Cut Ujong Village, West Aceh Regency. The Suak Puntong area is located at the top of the bathymetry image, while at the bottom right is the land of the Suak Puntong gampong.

In the case of this research, a bathymetric survey needs to be carried out to obtain depth data and visualization of the contour or topography of the bottom of the waters. The bathymetric survey includes the process of depicting the bottom of the waters starting from measurement, processing, to visualization of the bottom of the waters.

### 3.2 Wave Propagation in Suak Puntong

The wave distribution model modeled in this study is the wave model in Suak Puntong by carrying out 2 scenarios of different angles. The wave propagation model was carried out with 2 different scenarios, namely from the direction of the incident wave angle of  $180^\circ$ ,  $202.5^\circ$ .

The wave distribution model modeled in this case study is the wave distribution model in the Nagan Raya case study. Other parameters used are the direction of the incident wave ( $\alpha_0$ ) =  $180^\circ$  in meteorological coordinates, period  $T = 15$  seconds, height of the incident wave ( $H_0$ ) = 1.7 m. The results obtained show that the maximum wave height reached 3.5 m which occurred around the jetty.

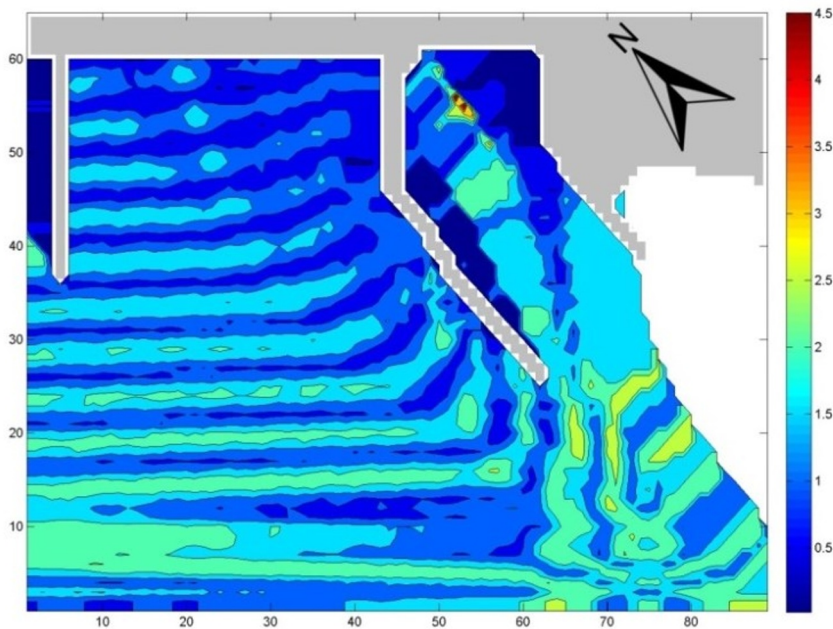


**Fig. 2.** Wave Propagation from an Incident Wave Angle of  $180^\circ$

The results obtained from the simulation of the wave ray propagation model in this case study were given a value of  $K_d$  (diffraction coefficient) of 0.5, and produced the image shown in **Figure 2** and wave ray profile shown in **Figure 3**. Another result shown for comparison is by looking at the wave height thinning beam profile. The point taken is at  $x = 50$  by looking at  $x = 50$  which experiences a deflection of waves towards the south due to the jetty and around the jetty the wave rays gather or accumulate so that the resulting wave energy is high.

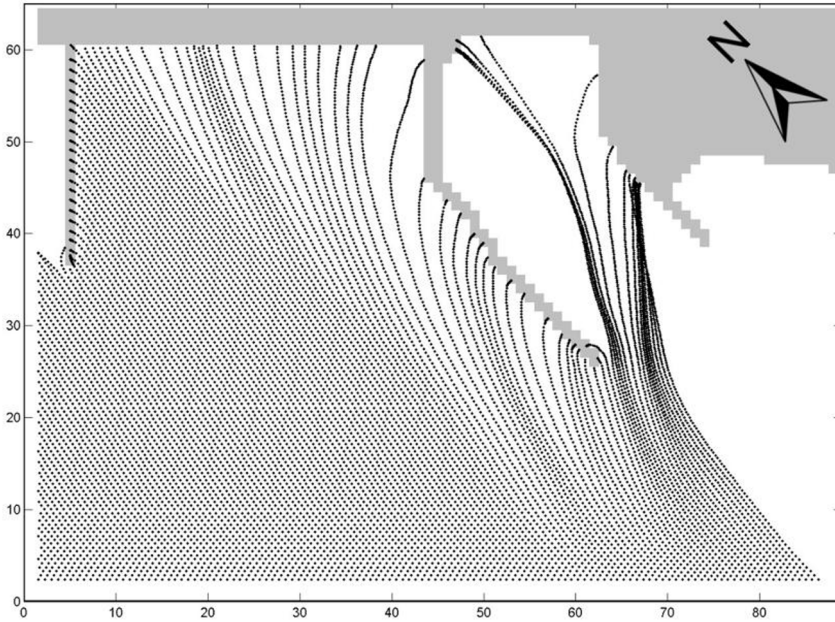


**Fig. 3.** Wave rays from an incident wave angle of  $180^\circ$

The wave distribution model modeled in this case study is the wave distribution model in the Nagan Raya case study. Another parameter used is the direction of the wave arrival ( $\alpha_0$ ) =  $202.5^\circ$  in meteorological coordinates, period  $T = 15$  seconds. The results obtained show that the maximum wave height reaches 4 m which occurs around the jetty.

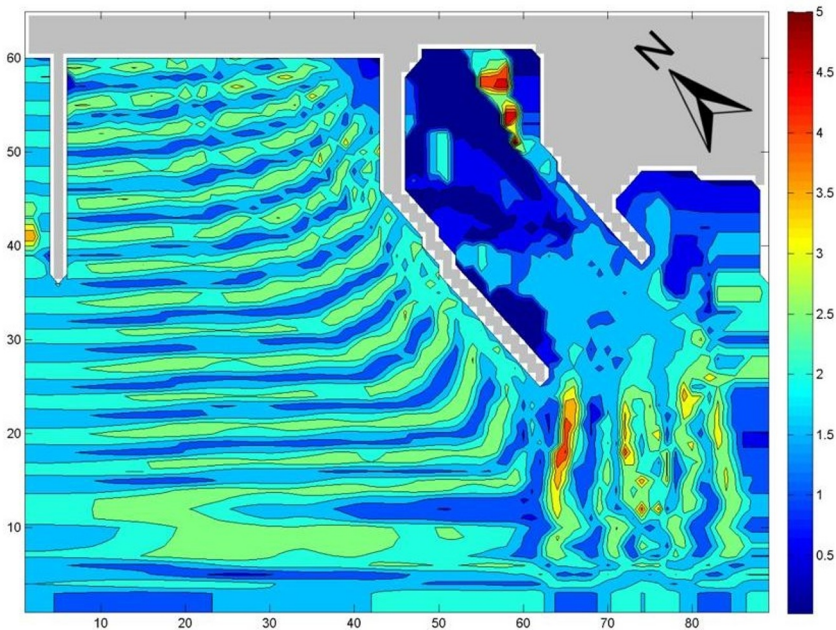


**Fig. 4.** Wave Propagation from an Incident Wave Angle of  $202.5^\circ$

The results obtained from the simulation of the wave ray propagation model in this case study were given a value of  $K_d$  (diffraction coefficient) of 0.5, and produced the image shown in **Figure 4** and wave ray profile shown in **Figure 5**. Another result shown for comparison is by looking at the wave height thinning beam profile. The point taken is at  $x = 50$  by looking at  $x = 50$  which experiences a deflection of waves towards the west due to the presence of a harbor and around the harbor the wave rays separate so that the wave energy produced is low.

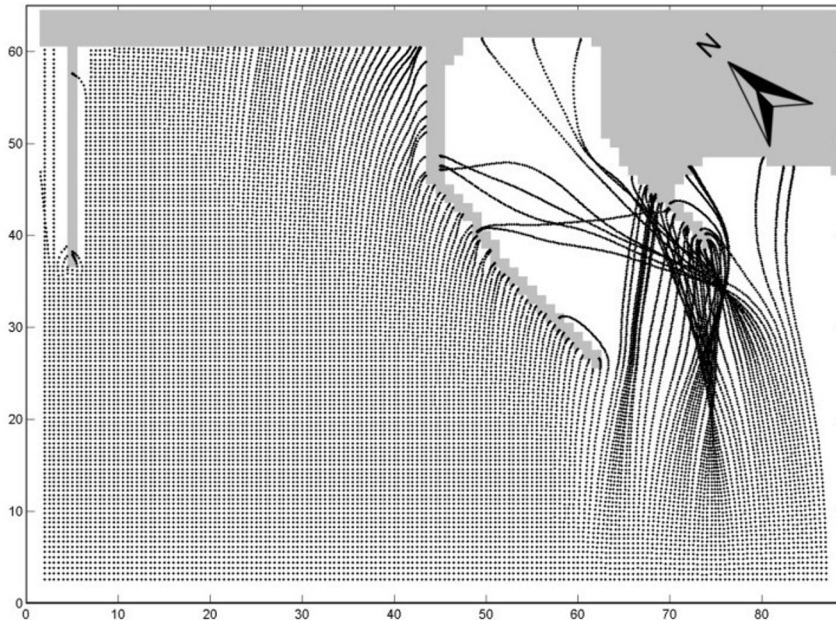


**Fig. 5.** Wave Rays from an Incident Wave Angle of  $202.5^\circ$

The results of the wave height propagation pattern show forms of refraction-diffraction equations. The highest waves occur in converging wave rays because they are close to the direction of the wave's incident angle and have a wave barrier in the form of a jetty. This undergoes a diffraction process so that the wave height is very high. This wave model is designed with an incident wave height of 2 m. This incoming wave height is taken from the average significant wave height from WaveWatch III (WW3) Global Wave Model data. Then the wave period value is also obtained from the average of the data. The wave height and period also indicate the stability of the waves in these waters.

In scenario I, wave height (m) with input of incident wave height ( $H_0$ ) = 1.7 m,  $T_p$  = 15 seconds, direction of the incident wave angle ( $\alpha_0$ ) =  $180^\circ$  (south). Where in this scenario a refraction process occurs because the wave bends towards the right. The wave rays in this scenario are directed away from each other and indicate a divergent zone. The wave height at an angle  $\alpha = 180^\circ$  shows that the highest wave profile with a height of up to 3.5 m occurs around the jetty. Scenario II, wave height (m) with input wave height ( $H_0$ ) = 1.7 m,  $T_p$  = 15 seconds, direction of the angle of incidence of the wave

### 3.3 Flow Model Result

The results of the flow distribution modeled in this study are currents caused by waves where these currents are greatly influenced by the size of the wave and the direction of the wave arrival. The direction of wave arrival is taken from the extreme direction of arrival towards the harbor at high tide and in the west season. The results of data collection in the field show

that the offshore incoming wave height is 1.7 meters with a period of 15 seconds from the southwest.

Judging from the current distribution conditions in the area around the port, it can be concluded that the current rotation is strong in the estuary area before entering the port pool, the current is concentrated and rotates at two points in the port pool (**Figure 6**). This occurs as a result of the depth (bathymetry) in the harbor pool being unequal (in one area being deep and in another area being shallow) thus causing instability in the current distribution.

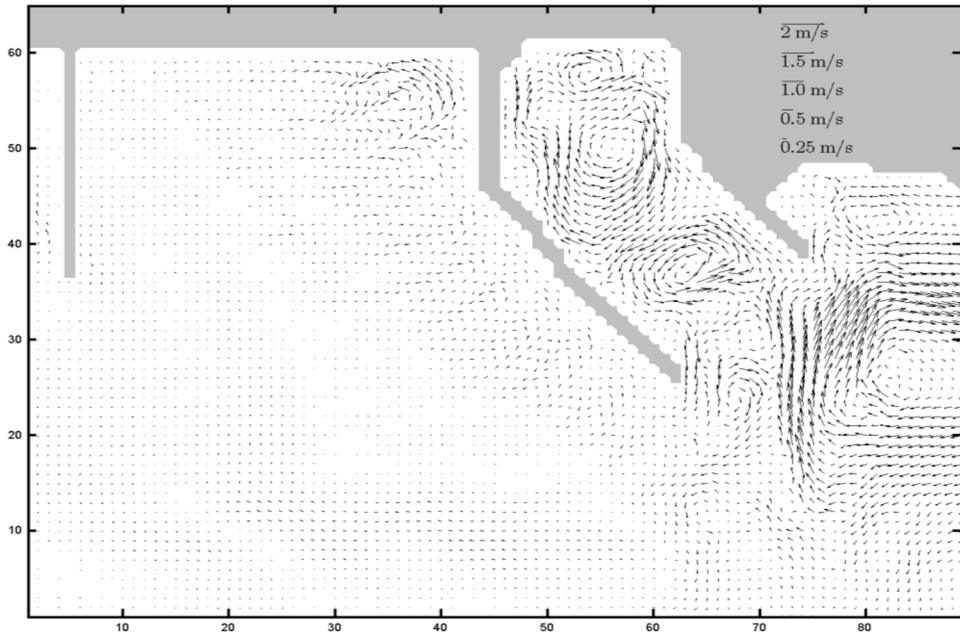


**Fig. 6.** Distribution of currents caused by waves in the study area.

## 4 Conclusion

Based on the results of research on wave propagation dynamics models in case studies in Gampong Suak Puntong, Kuala Pesisir District, Nagan Raya Regency, it shows that in scenario I, with the direction of the wave incident angle ( $\alpha 0$ ) = 180°,  $H_0$  = 1.7 m,  $T_p$  = 15 seconds. The bending waves separate from each other, which indicates a divergence zone and undergo a refraction process where the maximum wave height produced reaches 3.5 m. scenario II, with the direction of the incident wave angle ( $\alpha 0$ ) = 202.5°,  $H_0$  = 1.7 m,  $T_p$  = 15 seconds. The deflected waves overlap, which indicates a convergence zone and undergo a diffraction process where the maximum wave height produced reaches 4 m. So, in the two wave scenarios taken, there are wave refraction and diffraction phenomena.

## References

- [1] P. Nova, A. Pimenta-Martins, J. Laranjeira Silva, A. M. Silva, A. M. Gomes, and A. C. Freitas, *Crit. Rev. Food Sci. Nutr* **60(21)** 3680–3692 (2020)
- [2] M. Vikas and G. S. Dwarakish, *Aquat. Procedia*, **4** 381–388 (2015)
- [3] T. R. Walker *et al.*, “Environmental Effects of Marine Transportation,” in *World Seas: An Environmental Evaluation*, Elsevier, 2019, pp. 505–530.

- [4] N. I. Kadagi, N. Wambiji, S. T. Fennessy, M. S. Allen, and R. N. M. Ahrens, *Mar. Policy*, **124** 104351 (2021)
- [5] S. Wang, B. Lu, and K. Yin, *Mar. Policy*, **130** 104553 (2021)
- [6] S. C. Mohapatra, R. B. Fonseca, and C. Guedes Soares, *J. Coast. Res* **344** 928–938 (2018)
- [7] D. Justić *et al.*, *Estuaries and Coasts* **45(3)** 621–657 (2022)
- [8] H. Chen, X. Liu, and Q.-P. Zou, *Adv. Water Resour* **123** 160–172 (2019)
- [9] A. Mahmoodi, M. A. Lashteh Neshaei, A. Mansouri, and M. Shafai Bejestan, *J. Mar. Sci. Eng.*, **8(4)** 284 (2020)
- [10] R. Almar *et al.*, **12(1)** 3775 (2021)
- [11] M. Irham and I. Setiawan, *Omni-Akuatika*, **13(1)** (2017)
- [12] S.-I. Kang, W.-H. Ryang, and S.-S. Chun, *J. Korean earth Sci. Soc* **36(6)** 533–542 (2015)
- [13] E. R. Gomes, R. P. Mulligan, K. L. Brodie, and J. E. McNinch, *Coast. Eng* **116** 180–194 (2016)
- [14] V. A. Squire, *Philos. Trans. R. Soc. A Math. Phys. Eng. Sci.*, **376(2129)** 20170342, (2018)
- [15] I. Setiawan and M. Irham, *Civ. Eng. Dimens.*, **20(1)** 30–34 2018.
- [16] M. Irham, E. Miswar, Y. Ilhamsyah, and I. Setiawan, *IOP Conf. Ser. Mater. Sci. Eng.*, **352** 012043, (2018)
- [17] I. Setiawan, S. M. Yuni, S. Purnawan, Y. Ilhamsyah, and R. Wafdan, *IOP Conf. Ser. Earth Environ. Sci* **284(1)** 012026 (2019)
- [18] I. Setiawan *et al.*, *IOP Conf. Ser. Earth Environ. Sci* **176** 012016 (2018)
- [19] H. Zhang, W. Cheng, X. Qiu, X. Feng, and W. Gong, *Cont. Shelf Res* **142** 32–49 (2017)